A High-Performance Circularly-Polarized Rectenna for WirelessEnergy Harvesting at 1.85 and 2.45 GHz Frequency Band

Hakim Takhedmit, Zied Saddi, Laurent Cirio

Progress In Electromagnetics Research C, Vol. 79, 89–100, 2017

A High-Performance Circularly-Polarized Rectenna for Wireless Energy Harvesting at 1.85 and 2.45 GHz Frequency Bands

Hakim Takhedmit*, Zied Saddi, and Laurent Cirio

Abstract—This paper deals with the design and experiments of a dual-band circularly polarized rectenna at 1.85 and 2.45 GHz. It uses a single antenna and a single RF-to-dc rectifier. The circuit contains a dual-band circularly polarized antenna and a dual-band RF-to-dc rectifier based on a miniaturized 180° hybrid ring junction. The ring junction is used to independently match the sub-rectifiers at each frequency. The proposed rectenna was experimented with single-tone and multi-tone incident waves. It achieves more than 300 mV and 40% efficiency, across a 4-kΩ resistive load, at very low power density of 1.13 $\mu W/cm^2$ at 1.85 GHz and 1.87 $\mu W/cm^2$ at 2.45 GHz. It also achieves more than 150 mV under the same load condition and in the critical case when receiving only one of the two frequency bands. It is dedicated to harvest RF energy in the GSM 1800 and the 2.45-GHz ISM bands, regardless the polarization angle of the incident waves.

1. INTRODUCTION

Advances in wireless communications and low consumption electronics in recent decades have been followed by the growing proliferation of wireless devices like sensors, sensor nodes and actuators in different fields of application and at different locations. This raises the issue of their energy autonomy, especially since the power consumption of such devices is considered as the main obstacle before reaching the full mobility. The energy harvesting becomes increasingly an attractive solution for contactless powering of low-consumption electronic devices, particularly in the Internet of Things (IoT) and Machine-to-Machine (M2M) communications. It was recently demonstrated in [1, 2] that the ambient RF energy harvesting in urban and semi-urban environments can be competitive with other ambient sources, like thermal sources and mechanical vibrations. The RF power harvesting consists of capturing and then converting the ambient electromagnetic waves into useful dc power. The important element of such a system is called a rectenna, for rectifying antenna [2–6]. It contains a receiving antenna followed by a RF-to-dc rectifying circuit, terminated by a resistive load. The rectifier is often made up of a combination of Schottky diodes, an input HF filter and an output bypass capacitor. The output load models the input impedance of the device to be powered. The most important consideration for the rectenna design is how to achieve high output dc power. There are two main considerations to achieve this goal. First, maximum power should be collected by the antenna and delivered to the rectifying diode. Second, the high order harmonics created by the non linear behavior of the rectifier have to be confined around the diodes. Indeed, these harmonics must be filtered by the input HF filter in the RF side and by the output DC filter in the load side.

Most rectennas reported in the literature operate on a single frequency band [2–6] and their antennas are linearly polarized [2–4]. These rectennas are usually intended for Wireless Power Transfer (WPT). Indeed, in WPT the transmitting antenna is dedicated and its location is known. Moreover, the rectenna is in line of sight of the transmitter and the limitations in terms of EIRP (Equivalent Isotropically Radiated Power) are related to health considerations and are relatively high compared to the ambient

Received 7 July 2017, Accepted 18 October 2017, Scheduled 28 October 2017
* Corresponding author: Hakim Takhedmit (hakim.takhedmit@u-pem.fr).
The authors are with the Université Paris-Est. ESYCOM (EA 2552), CNAM, ESIEE Paris, UPEM, Marne-la-Vallée, France.

available RF power level. Besides, several spectral surveys of the ambient electromagnetic power [1, 7–10] in the urban environment show a low average power level and a power availability on several frequency bands, particularly those of mobile phone and Wi-Fi.

The aim of the paper is to harvest low electromagnetic power levels available in the environment, without knowing where the RF source is and how the incident wave is polarized. To increase the amount of RF power that the antenna could receive, the design of multi-band and broadband rectennas is a topic of some interest. Moreover, the circular polarization feature of the receiving antenna would make it possible to overcome the multipath and the depolarization waves issues. Indeed, a circularly polarized antenna captures a nearly constant power regardless the polarization of incident waves.

Some recent papers published in the literature deal with multi-band [1, 11, 12] and broadband [13] rectennas. Authors in [11] propose a tetra-band energy harvesting system, able to harvest RF energy from GSM 900, GSM 1800, UMTS and Wi-Fi sources available in the ambient. The circuit uses one rectifier, with multi-band matching network. A multi-band rectenna was proposed in [1] and prototypes were designed and fabricated for each band (DTV, GSM900, GSM1800, and 3G). The overall end-to-end efficiency of the prototypes using realistic input RF power sources is measured, an efficiency of 40% was obtained for the GSM900 prototype. A 64-element dual-circularly-polarized spiral rectenna array [13] is designed and characterized over a frequency range of 2–18 GHz with single-tone and multi-tone incident waves. Each rectenna element contains a broadband circularly polarized spiral antenna and a Schottky diode. The main challenges of such circuits are the impedance matching issue and the diode frequency-dependant efficiency. Indeed, the diode is a non-linear element. Its impedance depends on frequency, RF input power and output load. This makes the impedance matching between the rectifier and the antenna, over several bands or broadband, very challenging. One solution consists to use a radiating element and an RF-to-dc rectifier for each frequency band [14]. Multi-band impedance-matching networks [15, 16] were also used. These solutions are rather constraining, and they increase the complexity and dimensions of the device.

This paper deals with a novel dual-band circularly polarized rectenna topology operating at 1.85 and 2.45 GHz. The circuit uses a single antenna and a single conversion circuit. The idea consists to separate the inherent powers from the two frequency bands of interest and convert them using mono-band sub-rectifiers. The circuit does not use any dual band impedance matching network, which makes the design simple and efficient.

2. DESCRIPTION OF THE RECTENNA

The rectenna that we propose is shown in Fig. 1. It contains a dual-band circularly polarized (CP) antenna and a dual-band RF-to-dc rectifying circuit. It is etched in microstrip technology, on Arlon 25N substrate ($\varepsilon_r = 3.4$, $\tan\delta = 0.0025$, $h = 1.524$ mm) and operates at 1.85 and 2.45 GHz. The circular polarization is chosen in order to keep an almost constant received RF power level regardless the orientation of the antenna and the polarization of the incident electromagnetic wave. The antenna is printed on the ground plane, located on the top layer of the circuit. The conversion circuit, fed by a microstrip line, is printed on the bottom layer of the circuit.

2.1. Dual-Band Circularly Polarized Antenna

The receiving antenna contains two concentric annular ring slots, etched in the ground plane [17], and fed using a coupled microstrip line. It was designed and optimized under Ansys HFSS software. A short circuit of an angle θ_1 is placed on the outer slot (R_1 and W_1) to achieve circular polarization in the low frequency band at 1.85 GHz (GSM band). Besides, another short circuit of an angle θ_2 is placed on the inner slot (R_2 and W_2) to achieve circular polarization at the high frequency band at 2.45 GHz (ISM band). Circular polarization is possibly made by the two short circuits placed on the two slots, at 90° of the feeding line. The open stub (L_2, W_4) is tuned to cancel the reactance of the outer and the inner slots at 1.85 and 2.45 GHz, respectively. This maximizes the electromagnetic coupling with the feeding line. To achieve a 50-Ω impedance matching at 1.85 GHz, a quarter-wavelength transformer (L_1, W_3) is used. Moreover, the short circuit of an angle θ_2 is 5° rotated compared to that of angle θ_1. This allows providing 50-Ω impedance matching at 2.45 GHz.

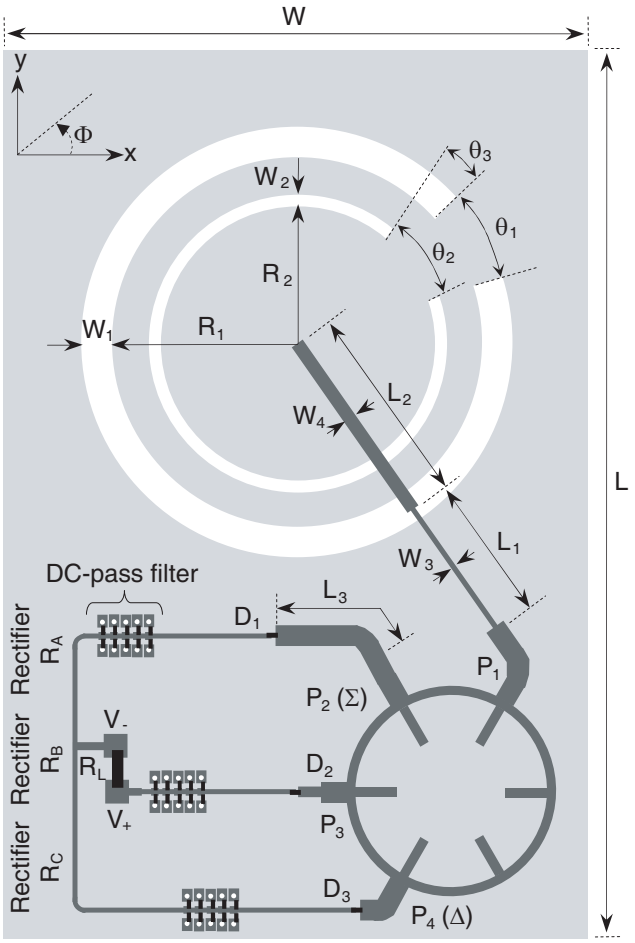

Figure 1. Layout of the proposed dual-band rectenna. $\theta_1 = 25°$, $\theta_2 = 34°$, $\theta_3 = 5°$, $R_1 = 32$, $R_2 = 23.5$, $W_1 = 5$, $W_2 = 1.5$, $L_1 = 24.8$, $L_2 = 34.5$, $L_3 = 21.5$, $W_3 = 1$, $W_4 = 2.2$, $L = 151$, $W = 100$ (all dimensions are in millimeters).

2.2. Dual Band RF-to-dc Rectifier

The RF-to-dc rectifying circuit is built around a miniaturized 180° hybrid ring junction [18]. The different accesses of the ring junction are denoted P_1 to P_4. Ports P_2 and P_4 are referred as the sum and difference accesses, respectively. The circuit contains three sub-rectifiers, denoted R_A, R_B and R_C. The sub-rectifiers R_A and R_C operate at 1.85 GHz and R_B at 2.45 GHz. Each sub-rectifier contains a single series-mounted SMS7630 Schottky diode [19], a lumped-elements dc-pass filter and an impedance matching stage. The Schottky diode is chosen for its low threshold voltage and shorter transit time, allowing high operating frequencies. All rectifiers are simulated and optimized under Advanced Design System software, by a co-simulation between Momentum electromagnetic simulator and Harmonic Balance circuit simulator. The frequency-dependant input impedance of the receiving antenna was calculated and exported from HFSS and used as the internal impedance of the power source in all Momentum/Harmonic Balance co-simulations. This allows an accurate modeling, taking into account the impedance of the antenna at different frequency components (fundamental and harmonics). The rectifier is intended to operate at low power levels of about −15 dBm, i.e., 31 µW. The sub-rectifiers outputs are interconnected by series and parallel dc recombinations to improve the voltage and the output power [20] compared to a single rectifier. Sub-rectifiers R_A and R_C are first connected in parallel, and then connected in series with the sub-rectifier R_B. The output dc voltage ($V_{dc} = V_+ - V_-$) is measured in a differential mode over an optimal resistive load (R_L) of 4 kΩ, without any contact with the ground plane.

2.2.1. Output dc-pass Filter

To block the RF power of the fundamental frequencies and harmonics, and then isolate the output resistive load from RF waves, each sub-rectifier contains a dc-pass filter. The filter, like shown in Fig. 2, contains 10 surface mounted capacitors of 100 pF. It has been simulated and optimized under Advanced Design System software. The transmission coefficient (S_{21}) of the filter is depicted in Fig. 3. It shows a transmission below −30 dB at the fundamental frequencies (1.85 and 2.45 GHz) and harmonics (3.7, 4.9, 5.55, 7.35 GHz. . .).

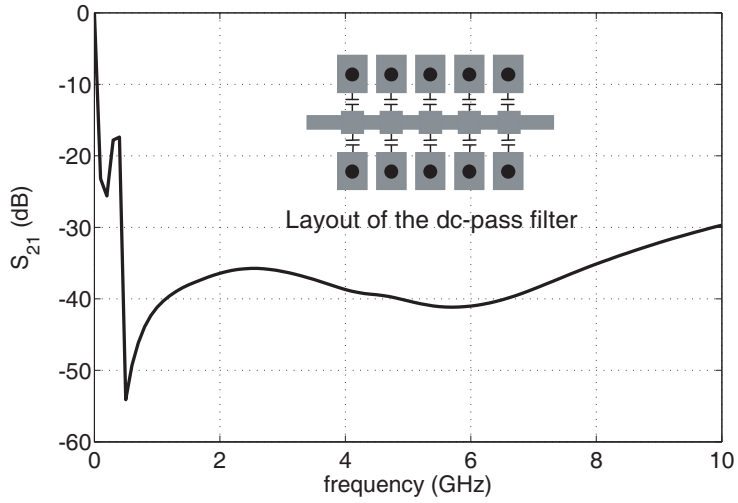

Figure 2. Transmission coefficient (S_{21}) of the dc-pass filter.

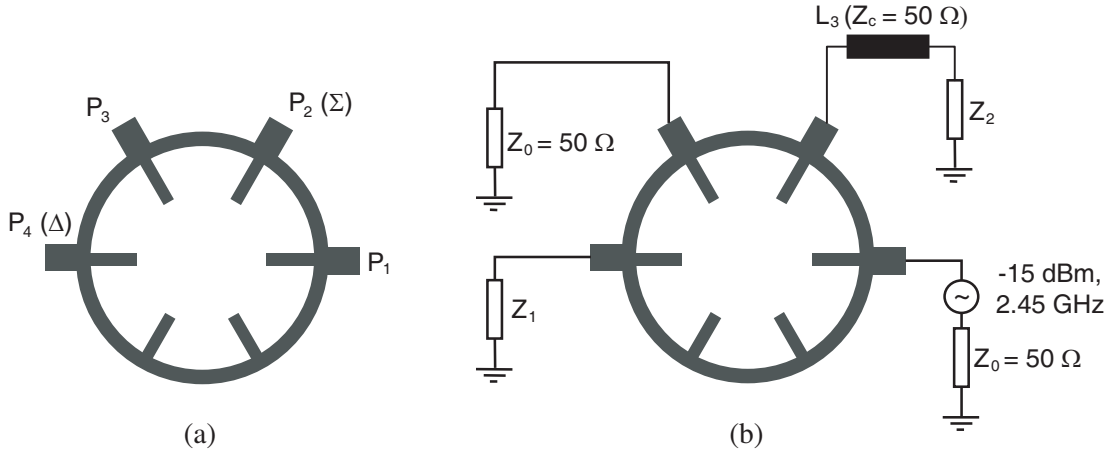

Figure 3. (a) Hybrid ring junction layout. (b) Optimization of the line length L_3.

2.2.2. Dual-Band Hybrid Ring Junction

The miniaturized 3 dB 180° hybrid ring junction, depicted in Fig. 3(a), is designed and optimized under Advanced Design System software, using the Momentum electromagnetic simulator. This circuit design is based on the work of M.-L. Chuang et al. [18]. It is miniaturized by the use of six open stubs, and operates at 1.85 and 2.45 GHz. The structure contains four accesses, denoted P_1 to P_4. If we consider that P_1 and P_3 are the inputs, P_2 and P_4 accesses are referred to be as the sum and the difference accesses, respectively.

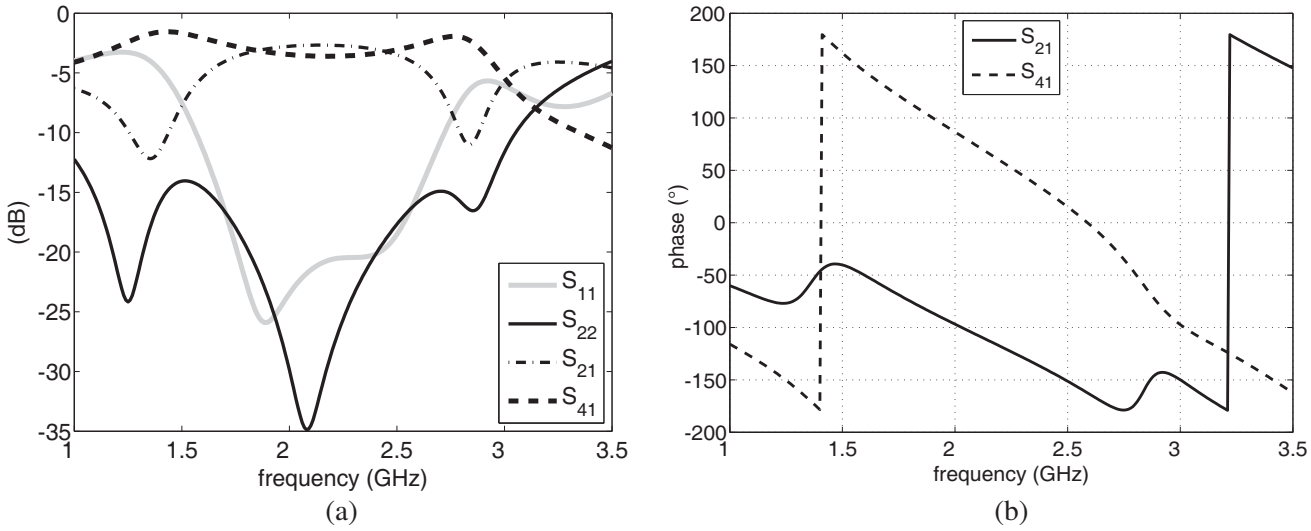

Figure 4. Simulated scattering parameters, (a) reflection and transmission coefficients, (b) phase difference between accesses P_2 and P_4, when P_1 is fed.

The simulated scattering parameters of the circuit within the frequency band ranging from 1 to 3.5 GHz are depicted in Fig. 4(a). Due to the symmetry of the circuit, only part of scattering parameters is considered: S_{11} and S_{22} for the reflection coefficients and S_{21} and S_{41} for the transmission coefficients. Results show that the accesses of the circuit are matched (< -20 dB) at the frequency bands of interest. The transmission coefficients S_{21} and S_{41} at 1.85 and 2.45 GHz are about 3 dB. The incident power from port 1 is equally divided between ports 2 and 4. Fig. 4(b) shows the phases of S_{21} and S_{41}. The phase difference between the accesses P_2 and P_4, when the port 1 is fed, is about 180° at the frequencies of interest.

The receiving antenna is connected to port P_1, considered as the input. The power received by the antenna at 1.85 GHz is split equally and transmitted to the accesses P_2 and P_4. The sub-rectifiers R_A and R_C, connected to these ports, are the same and operate at the frequency of 1.85 GHz. As these rectifiers are narrow band, they are strongly mismatched at the second frequency 2.45 GHz ($|\Gamma_{RA,RC \text{ at } 2.45\,GHz}| \approx 1$). Moreover, at 2.45 GHz it is sought to transmit all the power harvested by the antenna to the sub-circuit R_B, connected to the port P_3, which operates at this frequency. This requires a modification of the coupler. Indeed, the power captured by the antenna at 2.45 GHz would be divided into two entities, equal in amplitude and opposite in phase, and transmitted to the rectifiers R_A and R_C. As these rectifiers are mismatched at this frequency, each of the power entities will be fully reflected. Moreover, the lengths of lines between the accesses P_2 and P_3, and between P_4 and P_3 are the same. Therefore, the two powers resulting from these reflections arrive at the access P_3 with the same amplitude but opposite in phase, resulting in a zero power transmitted. The objective being to have all the power coming from the antenna, at the input of the rectifier R_B, a line L_3 has been added between the access P_2 and the rectifier R_A and its length has been tuned. As shown in Fig. 3(b), a 50-Ω microstrip line of length L_3 has been added to the port P_2 of the coupler. We used a -15 dBm/2.45 GHz source placed on the port P_1. The two ports P_3 and P_4 are loaded by the input impedance of the sub-rectifiers R_A and R_B, operating at the frequency of 1.85 GHz. We have used an s2p file for the input impedance of the sub-rectifiers R_A and R_B within the frequency band ranging from 0 to 10 GHz, including the fundamental frequency and the first harmonic. Fig. 5 depicts the transmitted power from the antenna (port P_1) to the sub-rectifier R_B (port P_3) depending on the line length L_3, from 15 to 30 mm. A maximum transmitted power of -15.28 dBm is obtained for a line length L_3 of 21.5 mm. This length is close to half wavelength. Indeed, it allows compensating for the path differences of 180° between the ports 2 and 4, when the port 1 is fed.

Based on scattering parameters, we will show that the RF power captured by the antenna (port P_1) at 2.45 GHz can be fully transmitted to the sub-rectifier R_B (port P_3) if the line L_3 is quarter

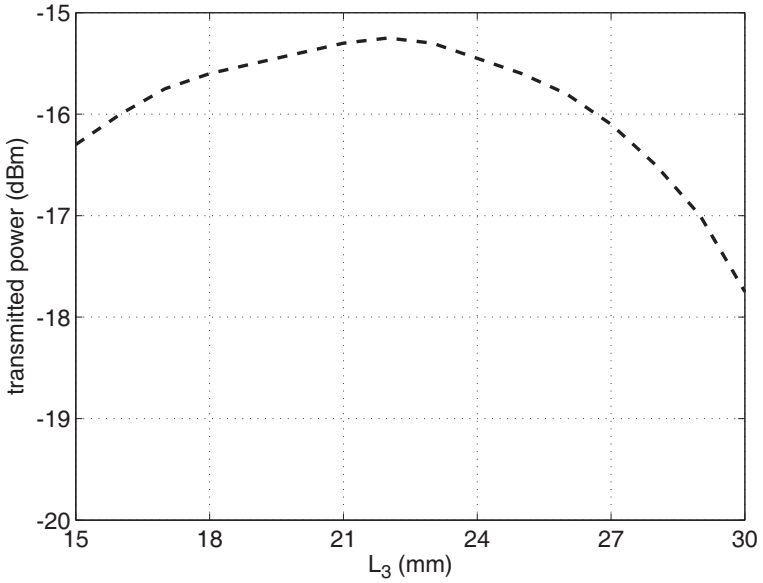

Figure 5. Transmitted power from the antenna to the sub-rectifier R_B against line length L_3.

wavelength and the sub-rectifiers R_A and R_C (ports P_2 and P_4) fully mismatched.

At 2.45 GHz, the scattering matrix of the hybrid ring junction including the quarter wavelength line section L_3 is given by:

$$S = -\frac{j}{\sqrt{2}} \begin{bmatrix} 0 & -j & 0 & -1 \\ -j & 0 & -j & 0 \\ 0 & -j & 0 & 1 \\ -1 & 0 & 1 & 0 \end{bmatrix} \tag{1}$$

We denote a_i and b_i ($i \in \{1, 2, 3, 4\}$) the incident and transmitted/reflected waves associated to the ports i of the hybrid ring junction, respectively. Γ is the reflection coefficient of sub-rectifiers R_A and R_C at 2.45 GHz ($|\Gamma| \approx 1$). For the sub-rectifiers R_A and R_C, a_2 and a_4 are considered as transmitted/reflected waves, b_2 and b_4 as incident waves. Then, the reflected waves (a_2 and a_4) from the sub-rectifiers can be expressed as a function of the incident waves (b_2 and b_4) and the input reflection coefficient (Γ) as follows:

$$a_2 = \Gamma b_2 \tag{2}$$

$$a_4 = \Gamma b_4 \tag{3}$$

From the scattering matrix in Eq. (1) given above, we can write:

$$b_3 = -\frac{j}{\sqrt{2}}(-ja_2 + a_4) \tag{4}$$

Substituting Eqs. (2) and (3) in Eq. (4) gives:

$$b_3 = -\frac{j}{\sqrt{2}}(-j\Gamma b_2 + \Gamma b_4) \tag{5}$$

From Eq. (1), b_2 and b_4 can be expressed as a function of a_1 and a_3. Equation (5) can then be rewritten as:

$$b_3 = \left(-\frac{j}{\sqrt{2}}\right)^2 [-j\Gamma(-ja_1 - ja_3) + \Gamma(-a_1 + a_3)] \tag{6}$$

and finally:

$$b_3 = \Gamma a_1 \tag{7}$$

Equation (7) shows that, if $|\Gamma|$ equals 1, then the transmitted power (b_3) to the sub-rectifier R_B will be equal to the power captured by the antenna (a_1).

3. SIMULATED AND EXPERIMENTAL RESULTS

A prototype of the dual-band circularly-polarized antenna was achieved, and measurements were performed to characterize it experimentally. Fig. 6 depicts the HFSS-simulated and measured reflection coefficient (S_{11}) within the frequency band ranging from 1.6 to 2.8 GHz. One can observe a good impedance matching on the two bands of interest and a good agreement between simulated results and those measured. Although, slight frequency shifts can be observed. This is mainly due to the fabrication and measurements tolerances. Input reflection coefficient values of -16 and -14 dB are experimentally obtained at 1.85 and 2.45 GHz, respectively. Simulation shows -15.6 and -16.4 dB at the same frequencies. The simulated and measured axial ratios are shown in Fig. 7. The HFSS simulation gives an axial ratio of 0.9 dB at 1.85 and 2.45 GHz. The measurements show an axial ratio of 1.5 dB in the low frequency band and 0.78 dB in the high frequency band, although there are 40 and 20 MHz shifts to lower frequencies, compared with the simulation. Fig. 8 shows a comparison between the simulated and measured circular-polarization gains in the two frequency bands of interest. There is good agreement between the simulated gain curves and those obtained by measurements. Table 1 gives some CP gain values at relevant frequencies. At 1.85 GHz, the simulated CP gain is 4.54 dBic, and the measured one is 4.08 dBic. At 2.45 GHz, the simulated and measured CP gains are 4.64 and 3.94 dBic, respectively.

Table 1. Simulated and measured CP gains values at some relevant frequencies.

Frequency (GHz)	**1.81**	**1.83**	**1.85**	**2.41**	**2.42**	**2.45**
Simulated gain (dBic)	4.4	4.5	4.54	4.79	4.77	4.64
Measured gain (dBic)	4.09	4	4.08	4.49	4.42	3.94

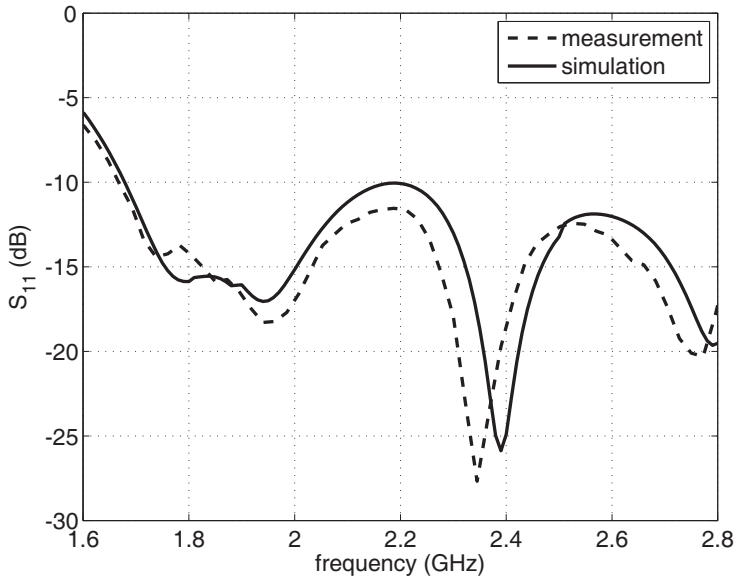

Figure 6. Input reflection coefficient of the antenna versus frequency.

The dual-band RF-to-dc rectifier was also fabricated and measured. The circuit was fed by a two-tone RF source, the frequency and the power are tunable. The output voltage is measured by a voltmeter at the terminals of the resistive load R_L placed at the end of the rectifier (Fig. 1). Measured output voltage of 46 and 1120 mV are obtained at -25 and -5 dBm, respectively. The output load is optimal and set to 4 kΩ. The related conversion efficiency values are 8.5 and 50%.

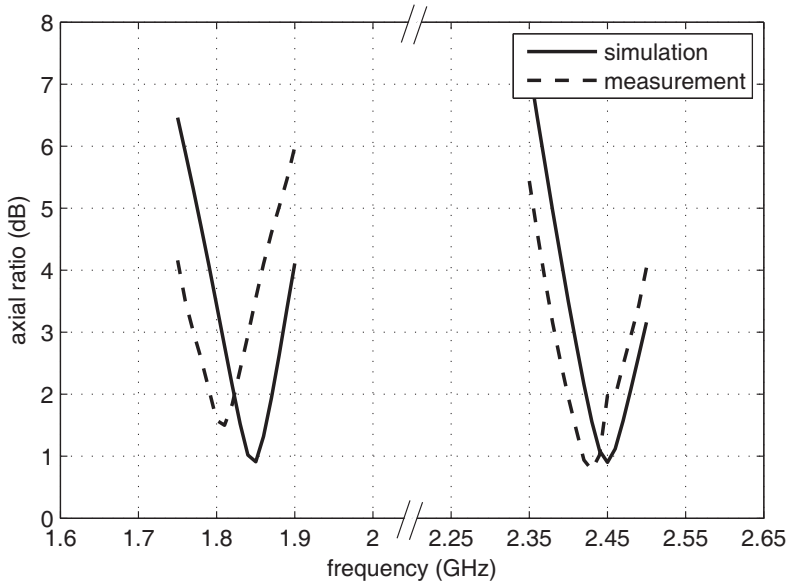

Figure 7. Simulated and measured axial ratio against frequency.

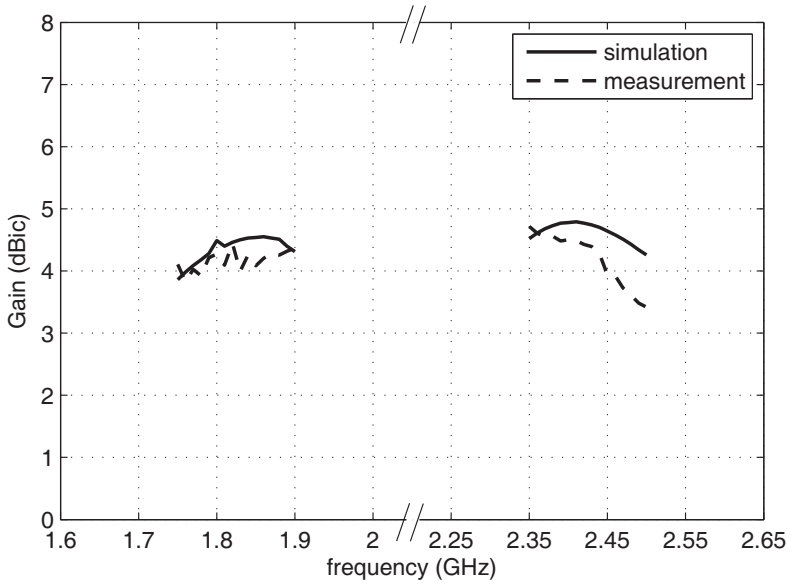

Figure 8. Comparison between simulated and measured CP gains.

A prototype of the full rectenna was fabricated and characterized inside an anechoic chamber. The measurement setup is shown in Fig. 9. It contains a transmitting horn antenna (BBHA 9120B of Schwarzbeck Mess-Elecktronik), two RF sources (E8251A and 83623A of Agilent), a power amplifier (20S1G4 of AR), a power combiner, a hybrid coupler and a spectrum analyzer (FSEA30 of Rohde & Schwarz). A conventional voltmeter is used to measure the output dc voltage ($V_{\mathrm{dc}} = V_{+} - V_{-}$) across the resistive load (R_L). The far field distance requirement at 1.85 GHz is located at about 50 cm from the transmitting horn antenna. The rectenna under test is then placed in the far field region at a distance (d) of 1.5 m from a transmitting horn antenna. The rectenna can be illuminated by a one- or two-tones electromagnetic waves. The RF input powers delivered by the RF generator are accurately estimated such that a power of -15 dBm at 1.85 GHz and -15 dBm at 2.45 GHz will be captured by the dual-

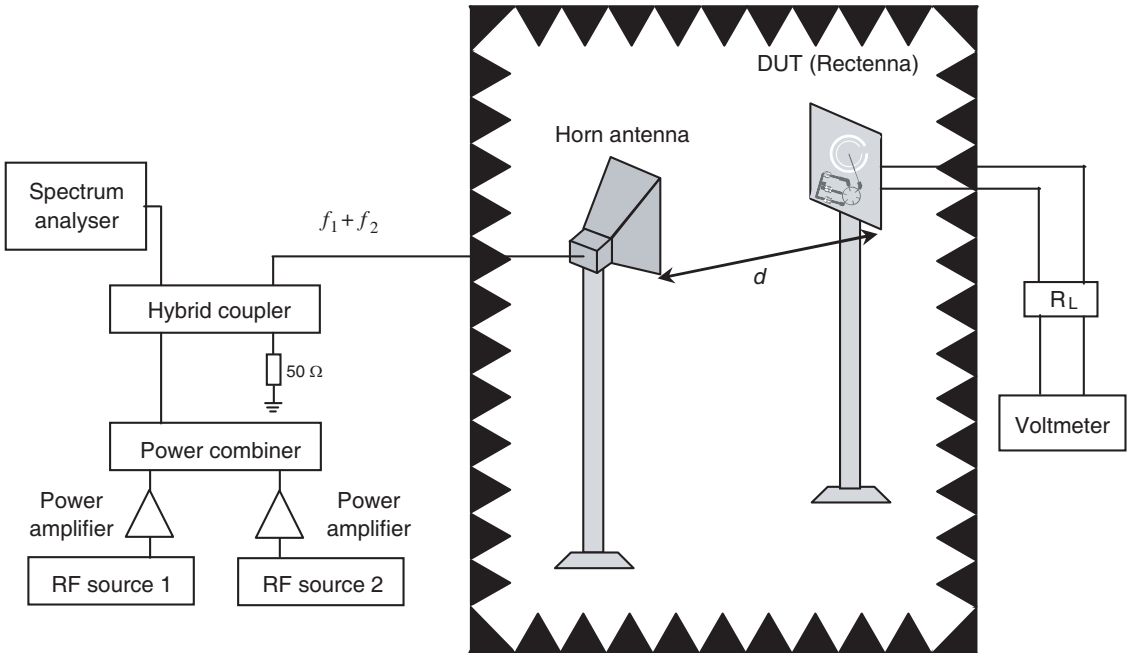

Figure 9. Measurement setup.

band antenna and transmitted to the rectifier circuit. Measurements as a function of the frequency, in the two bands of interest, were achieved and results are depicted in Fig. 10. When the rectenna is illuminated by two-tone electromagnetic waves at −15 dBm per tone, it delivers more than 300 mV voltage on an optimal load of 4 kΩ. In the extreme case where the rectenna receives −15 dBm on one of the two frequency bands, the output voltage is greater than 150 mV in the same load conditions. Indeed, the sub-rectifiers operating at 1.85 GHz and those operating at 2.45 GHz are connected in series as illustrated in Fig. 1. Each of them acts as a dc generator and contribute to the output voltage. The results show that there is little influence from one part to the other. The rectenna is intended to harvest electromagnetic waves on the two frequency bands. However, it keeps perfectly adequate performance when the power is captured on one of the two bands. This shows a robustness with respect to the power imbalances and its extreme when the power on one of the two bands is zero.

Also, measurements as a function of power density were conducted for several azimuthal angles (Φ). Results are presented in Fig. 11. The dc voltage ($V_{\rm dc}$) and efficiency (η) are depicted as a function of ρ_1 and ρ_2, the power densities at 1.85 GHz and 2.45 GHz. ρ_1 and ρ_2 have been adjusted to receive the same RF power on the two frequencies of interest. The rectenna efficiency is defined as the ratio between the output dc power and the total captured RF power and is given by:

$$\eta\,(\%) = 100 \cdot \frac{\frac{V_{dc}^2}{R_L}}{P_{RF1} + P_{RF2}} \tag{8}$$

where $V_{\rm dc}$ is the dc output voltage measured over the resistive load R_L, and $P_{\rm RF1}$ and $P_{\rm RF2}$ are the available RF powers in the two frequency bands GSM 1800 MHz and ISM 2.45 GHz. These RF powers can be estimated with the following relationship:

$$P_{\rm RF1,2} = \rho_{r,2} \times A_{e1,2} \tag{9}$$

where $\rho_{1,2}$ and $A_{e1,2}$ are the power densities and the effective apertures of the antenna at 1.85 and 2.45 GHz.

The different curves for different azimuthal angles ($\Phi = -90°$, $-45°$, $0°$, $45°$ and $90°$) are close to each other. This shows that the power received by the antenna varies little with the Φ-angle variation. These results also indicate a good quality of circular polarization at frequencies of interest. The efficiency ripple, defined as the ratio between the maximum and minimum efficiencies, slightly

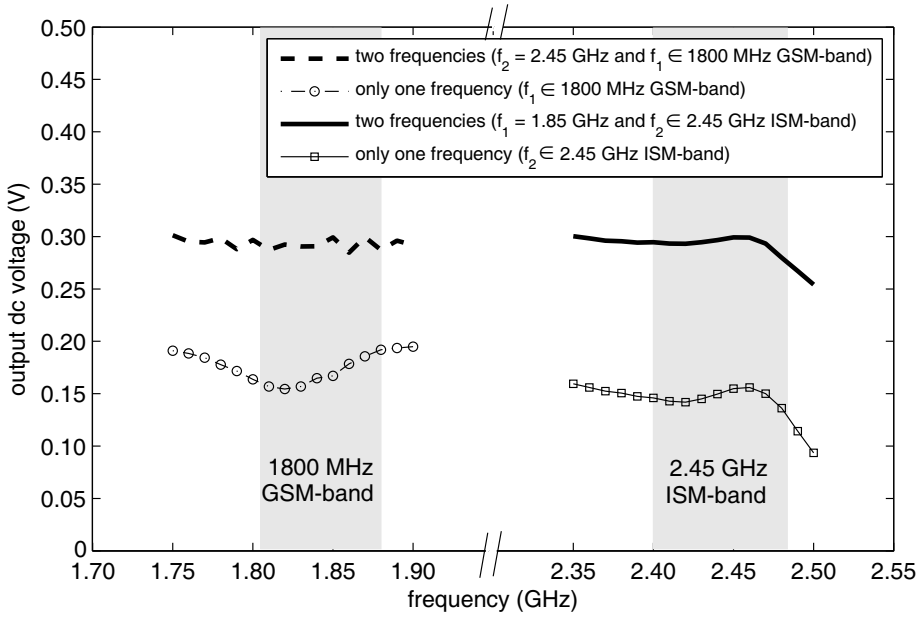

Figure 10. Measured output dc voltage of the rectenna against frequency.

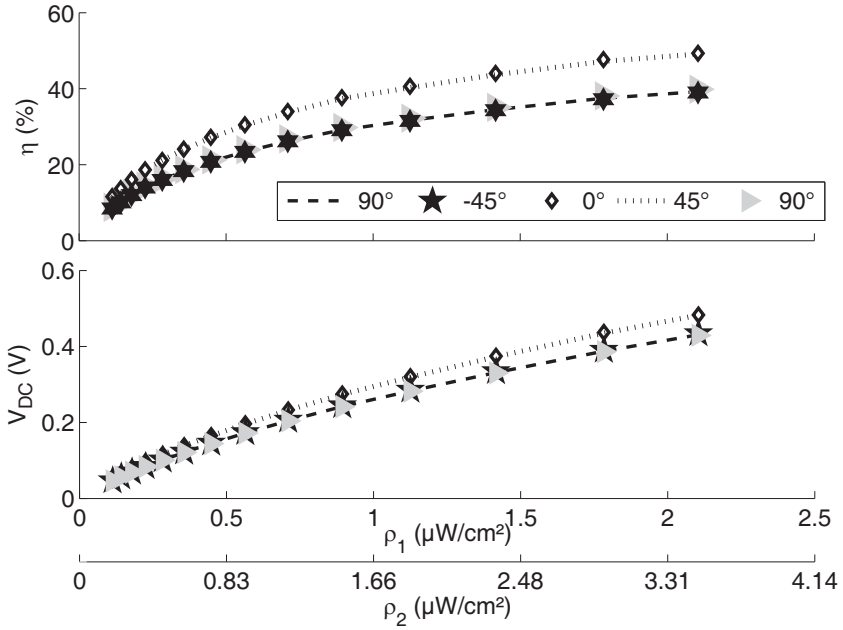

Figure 11. Measured output dc voltage and efficiency of the rectenna against power density, for several azimuthal angles ($\Phi = -90°$, $-45°$, $0°$, $45°$ and $90°$).

varies between 0.9 and 1.2 dB. It can also be seen that the dc output increases when the power densities ρ_1 and ρ_2 increase. When ρ_1 and ρ_2 are respectively set to $1.13\,\mu W/cm^2$ ($E_{rms} = 2\,V/m$) and $1.87\,\mu W/cm^2$ ($E_{rms} = 2.66\,V/m$), which corresponds to an RF power of -15 dBm at both 1.85 and 2.45 GHz, measurements show a dc voltage and efficiency of 320 mV and 40.6%. A maximum measured efficiency of about 50% ($V_{dc} = 485\,mV$) is obtained when ρ_1 and ρ_2 are respectively set to $2.1\,\mu W/cm^2$ ($E_{rms} = 2.8\,V/m$) and $3.5\,\mu W/cm^2$ ($E_{rms} = 3.6\,V/m$).

4. CONCLUSION

The design and experiments of a novel dual-band circularly polarized rectenna operating in the 1800-MHz GSM-band and 2450-MHz ISM-band are reported in this paper. The rectenna contains a single antenna and a single rectifier. The antenna contains two concentric annular ring slots etched in the ground plane. The rectifier contains three sub-rectifiers, based on Schottky diodes and a miniaturized 180° hybrid ring junction, used to separate the 1.85 and 2.45 GHz signals. This circuit overcomes the dual-band input impedance matching network and makes the structure simple and efficient. It experimentally achieves 320 mV of voltage and 40.6% efficiency when the power densities are 1.13 and 1.87 $\mu W/cm^2$ at 1.85 and 2.45 GHz, respectively. The rectenna is insensitive to polarization of incident plane waves and shows a very low efficiency ripple at 1.85 and 2.45 GHz. This rectenna is intended to harvest very low RF power densities and is well suited for remote powering of autonomous wireless sensors and actuators.

REFERENCES

1. Pinuela, M., P. D. Mitcheson, and O. Lucyszyn, "Ambient RF energy harvesting in urban and semi-urban environments," *IEEE Transactions on Microwave Theory and Techniques*, Vol. 61, No. 7, 2715–2726, May 2013.
2. Olgun, U., C.-C. Chen, and J. L. Volakis, "Design of an efficient ambient WiFi energy harvesting system," *IET Microwaves, Antennas & Propagation*, Vol. 6, No. 11, 1200–1206, Aug. 2012.
3. Takhedmit, H., L. Cirio, O. Picon, C. Vollaire, B. Allard, F. Costa, and O. Picon, "Design and characterization of an efficient dual patch rectenna for microwave energy recycling in the ISM band," *Progress In Electromagnetics Research C*, Vol. 43, 93–108, 2013.
4. Takhedmit, H., L. Cirio, B. Merabet, B. Allard, F. Costa, C. Vollaire, and O. Picon, "Efficient 2.45 GHz rectenna design including harmonic rejecting rectifier device, *Electronics Letters*, Vol. 46, No. 12, 811–812, Jun. 2010.
5. Takhedmit, H., L. Cirio, S. Bellal, D. Delcroix, and O. Picon, "Compact and efficient 2.45 GHz circularly polarised shorted ring-slot rectenna," *Electronics Letters*, Vol. 48, No. 5, 253–254, Mar. 2012.
6. Haboubi, W., H. Takhedmit, J. D. Lan Sun Luk, S. E. Adami, B. Allard, F. Costa, C. Vollaire, O. Picon, and L Cirio, "An efficient dual-circularly polarized rectenna for RF energy harvesting in the 2.45 GHz ISM band," *Progress In Electromagnetics Research*, Vol. 148, 31–3, 2014.
7. French Radio-Frequency Agency 'ANFR', https://www.cartoradio.fr/cartoradio/web/.
8. Mikeka, C., H. Arai, A. Georgiadis, and A. Collado, "DTV band micropower RF energy-harvesting circuit architecture and performance analysis," *IEEE Int. RFID-Technol. Appl. Conf.*, 561–567, 2011.
9. Song, C., Y. Huang, J. Zhou, J. Zhang, S. Yuan, and P. Carter, "A high-efficiency broadband rectenna for ambient wireless energy harvesting," *IEEE Transactions on Antennas and Propagation*, Vol. 63, No. 8, 3486–3495, Aug. 2015.
10. Mimis, K., D. Gibbins, S. Dumanli, and G. T. Watkins, "Ambient RF energy harvesting trial in domestic settings," *IET Microwaves Antennas & Propagation*, Vol. 9, No. 5, 454–462, Apr. 2015.
11. Masotti, D., A. Costanzo, M. Del Prete, and V. Rizzoli, "Genetic-based design of a tetra-band high-efficiency radio-frequency energy harvesting system," *IET Microwaves, Antennas & Propagation*, Vol. 7, No. 15, 1254–1263, 2013.
12. Costanzo, F., F. Donzelli, D. Mazotti, and V. Rizzoli, "Rigorous design of RF multi-resonator power harvesters," *European Conference on Antennas and Propagation*, 1–4, Apr. 2010.
13. Hagerty, J. A., F. B. Helmbrecht, W. H. McCalpin, R. Zane, and Z. Popovic, "Recycling ambient microwave energy with broad-band rectenna arrays," *IEEE Transactions on Microwave Theory and Techniques*, Vol. 52, No. 3, 1014–1024, Mar. 2004.
14. Heikkinen, J. and M. Kivikovski, "A novel dual-frequency circularly polarized rectenna," *IEEE Antennas and Wireless Propag. Letters*, Vol. 2, No. 1, 330–333, 2003.

15. Ren, Y. J., M. F. Farooqui, and K. Chang, "A compact dual-frequency rectifying antenna with high-order harmonic-rejection," *IEEE Transactions on Antennas and Propagation*, Vol. 55, No. 7, 2110–2113, Jul. 2007.
16. Suh, Y. H. and K. Chang, "A high-efficiency dual-frequency rectenna for 2.45- and 5.8-GHz wireless power transmission," *IEEE Transactions on Microwave Theory and Techniques*, Vol. 50, No. 7, 1784–1789, Jul. 2002.
17. Chen, L. T., J. F. Tsai, M. J. Hou, and J. S. Row, "Dual-band circularly polarized annular ring slot antenna," *Proceedings of Microwave Conference (APMC)*, 46–48, Dec. 2012.
18. Chuang, M. L. and M. T. Wu, "Miniaturized ring coupler using multiple open stubs," *Microwave and Optical Technology Letters*, Vol. 42, No. 5, 379–383, Jul. 2004.
19. Datasheet: "Surface mount mixer and detector Schottky diodes Skyworks," http:/www.skyworksinc.com.
20. Takhedmit, H., L. Cirio, B. Merabet, B. Allard, F. Costa, C. Vollaire, and O. Picon, "A 2.45-GHz dual-diode rectenna and rectenna arrays for wireless remote supply applications," *Intern. Journal of Microw. and Wireless Technologies*, Vol. 3, No. 3, 251–258, Jun. 2011.